Stem Cell Reports
Article

ISSCR

OPEN ACCESS

Extension of retinofugal projections in an assembled model of human pluripotent stem cell-derived organoids

Clarisse M. Fligor,[1] Sailee S. Lavekar,[1] Jade Harkin,[2,3] Priya K. Shields,[1] Kirstin B. VanderWall,[1] Kang-Chieh Huang,[1] Cátia Gomes,[4,5] and Jason S. Meyer[3,4,5,6,7,*]

[1]Department of Biology, Indiana University Purdue University Indianapolis, Indianapolis IN, USA
[2]Interdisciplinary Biomedical Research Gateway Program, Indiana University School of Medicine, Indianapolis IN, USA
[3]Department of Pharmacology and Toxicology, Indiana University School of Medicine, Indianapolis IN, USA
[4]Department of Medical and Molecular Genetics, Indiana University School of Medicine, Indianapolis IN, USA
[5]Stark Neurosciences Research Institute, Indiana University School of Medicine, Indianapolis IN, USA
[6]Department of Ophthalmology, Indiana University School of Medicine, Indianapolis IN, USA
[7]Twitter: @meyerlab
*Correspondence: meyerjas@iu.edu
https://doi.org/10.1016/j.stemcr.2021.05.009

SUMMARY

The development of the visual system involves the coordination of spatial and temporal events to specify the organization of varied cell types, including the elongation of axons from retinal ganglion cells (RGCs) to post-synaptic targets in the brain. Retinal organoids recapitulate many features of retinal development, yet have lacked downstream targets into which RGC axons extend, limiting the ability to model projections of the human visual system. To address these issues, retinal organoids were generated and organized into an *in vitro* assembloid model of the visual system with cortical and thalamic organoids. RGCs responded to environmental cues and extended axons deep into assembloids, modeling the projections of the visual system. In addition, RGC survival was enhanced in long-term assembloids, overcoming prior limitations of retinal organoids in which RGCs are lost. Overall, these approaches will facilitate studies of human visual system development, as well as diseases or injuries to this critical pathway.

INTRODUCTION

Three-dimensional organoids derived from human pluripotent stem cells (hPSCs) have revolutionized the ability to model the development of human tissues, closely recapitulating both the spatial and the temporal differentiation of cell types (Ader and Tanaka, 2014; Brown et al., 2018; Lancaster and Knoblich, 2014; Quadrato and Arlotta, 2017). Among the tissues to be modeled with organoids, retinal organoids closely model the stratification of all of the major cell types of the retina (Lu and Barnstable, 2019; Sridhar et al., 2018), including the organization of photoreceptors in apical layers and retinal ganglion cells (RGCs) found within basal layers. This spatiotemporal organization of retinal organoids has resulted in their use for studies related to human retinogenesis (Capowski et al., 2019; Cowan et al., 2020; Eldred et al., 2018; Fligor et al., 2018; Kallman et al., 2020; Sridhar et al., 2020; Wahlin et al., 2017; Zhong et al., 2014), as well as diseases resulting in the degeneration of retinal neurons (Huang et al., 2019; Lane et al., 2020; Parfitt et al., 2016; VanderWall et al., 2020a).

Many studies of retinal organoids to date have focused on the development of photoreceptors, as well as those diseases that adversely affect these cells (Eldred et al., 2018; Kallman et al., 2020; Wahlin et al., 2017; Zhong et al., 2014). Conversely, studies of RGCs within retinal organoids have received considerably less attention, likely due to a lesser organization of these cells within organoids as well as their eventual loss within long-term cultures, limiting the applicability of retinal organoids for diseases affecting RGCs. As the projection neurons of the visual system, RGCs serve as the sole connection between the eye and the brain (Crair and Mason, 2016). The ability to study RGC axonal outgrowth within three-dimensional organoid cultures would significantly add to our understanding of the development and pathfinding of these critical cell types, and would also provide a powerful model for the analysis of diseases affecting RGCs as well as a tool for studying strategies to encourage the regeneration of RGC axons.

Among the possible explanations for the loss of RGCs within retinal organoids, the neurotrophic hypothesis states that RGCs require essential survival signals from post-synaptic targets for their survival (Northcutt, 1989; von Bartheld et al., 1996). In the absence of these survival factors, RGCs undergo apoptosis. As these post-synaptic targets are found largely within the thalamic regions of the brain, traditional retinal organoid cultures do not account for the necessity of post-synaptic targets and, thus, RGCs lack these vital pro-survival factors leading to their degeneration.

To address these shortcomings, the current study focuses upon three-dimensional assembloids as a powerful approach to study the enhanced survival of stem cell-derived RGCs as well as the mechanisms underlying the long-distance projection of RGC axons toward

 © 2021 The Author(s).
This is an open access article under the CC BY-NC-ND license (http://creativecommons.org/licenses/by-nc-nd/4.0/).

physiologically relevant tissues. Generated from the fusion of regionally patterned individual organoids, assembloids effectively model the projections between distinct regions of the nervous system (Amin and Paşca, 2018; Chen et al., 2020; Miura et al., 2020; Xiang et al., 2019). To model the outgrowth of RGC axons into the brain, initial efforts explored the fusion of retinal and brain organoids to provide RGCs with brain-like tissue for the study of RGC projections. Subsequently, assembloids were generated to join retinal, thalamic, and cortical organoids. Within these assembloids, RGCs extended long-distance axons and exhibited enhanced survival compared with those grown in retinal organoids alone. The results of these studies are an important step toward re-creating retinotectal projections in a dish and represent a novel platform for studying the development of human RGCs as well as a more physiologically relevant system for analyses of how RGCs are lost in neurodegenerative diseases such as glaucoma.

RESULTS

hPSC-derived RGCs respond to environmental cues

During the development of the visual system, RGC axons are required to accurately survey their environment and respond to a variety of cues to reach their post-synaptic targets (Murcia-Belmonte and Erskine, 2019). To determine if hPSC-derived RGCs were similarly capable of responding to extrinsic signals, RGCs were differentiated from hPSCs through the generation of three-dimensional retinal organoids and subsequent purification of RGCs by sorting for the tdTomato:Thy1.2 reporter (Sluch et al., 2017; VanderWall et al., 2019, 2020a). By 45 days of differentiation, RGCs were readily identified within retinal organoids based upon the expression of tdTomato (Figures 1A–1C). Mimicking the lamination of the human retina, RGCs were observed exclusively within the inner layers of retinal organoids, as opposed to the localization of photoreceptors in outer layers. Following the enzymatic dissociation of retinal organoids and subsequent purification of RGCs by sorting for the Thy1.2 cell surface antigen, elaborate axons were observed surveying the environment with F-actin-enriched growth cones at the leading edge of each axon (Figure 1D). Thus, ensuing experiments explored the ability of RGC axons to appropriately respond to environmental cues.

Purified RGCs were seeded into microfluidic devices to document axonal outgrowth over time and in response to external stimuli (Figure 1E). Compared with those cultures grown in medium alone, RGCs extended significantly more axons crossing into the contralateral chamber when the axonal compartment was supplemented with brain-derived neurotrophic factor (BDNF) (Figures 1F–1H). Similarly, the supplementation of BDNF in the axonal chamber resulted in an increase in neurite complexity of cell bodies within the soma chamber (Figures 1I–1K). Thus, these experiments demonstrated the ability of hPSC-derived RGC axons to appropriately respond to environmental stimuli.

Next, to assess the ability of hPSC-derived RGCs to respond to signals from a physiologically relevant tissue, co-culture explant experiments were designed. The lateral geniculate nucleus (LGN) is a primary post-synaptic target of RGCs (Murcia-Belmonte and Erskine, 2019) and thus, explant cultures of mouse LGN tissue were established (Figure S1). Subsequently, hPSC-derived RGCs were grown either alone or in co-culture with explants of tissue from the mouse LGN (Figures 2A and 2B). As a control, co-cultures were also established between hPSC-derived RGCs and explants of mouse olfactory bulb, serving as an easily accessible brain tissue that would not be an appropriate target for RGCs (Figure 2C). The average neurite length of RGCs co-cultured with LGN explants was significantly increased compared with control RGCs cultured alone, with the presence of an olfactory bulb explant showing no discernable effect on neurite outgrowth (Figure 2D). Subsequently, Sholl analyses demonstrated that RGCs co-cultured with LGN explants extended significantly more neurites, with an increased number of neurites reaching the target, compared with those RGCs grown in co-culture with olfactory bulb (Figures 2E and 2F), suggesting that the presence of LGN-derived factors influences the degree of RGC axonal outgrowth. After 1 week in culture, RGC axons oriented toward the LGN were significantly longer compared with axons in the same orientation toward olfactory bulb co-cultures, as well as control RGCs grown alone (Figures 2G–2K), suggesting that an appropriate post-synaptic target influences the directionality of RGC axonal outgrowth. Overall, these experiments demonstrated that axonal outgrowth from hPSC-derived RGCs could be influenced by extrinsic signals, not only increasing the length of RGC axons but also influencing the directionality of axonal outgrowth.

Generation of retinal and brain assembloids to analyze RGC axonal outgrowth

During embryonic development, the retina is derived as an outgrowth from the diencephalic region of the neural tube and remains physically connected to the brain through axonal projections of RGCs (Murcia-Belmonte and Erskine, 2019). Given the close proximity in which the retina and brain are derived, it is perhaps not surprising that differentiation protocols to derive retinal organoids have often identified parallel populations reminiscent of developing prosencephalic structures (Meyer et al., 2011; Sridhar et al., 2013; Zhong et al., 2014). Thus, the ability to utilize retinal and prosencephalic brain organoids to generate assembloids for the study of RGC axonal outgrowth was further explored (Figures 3A and 3B). After 50 days of total differentiation,

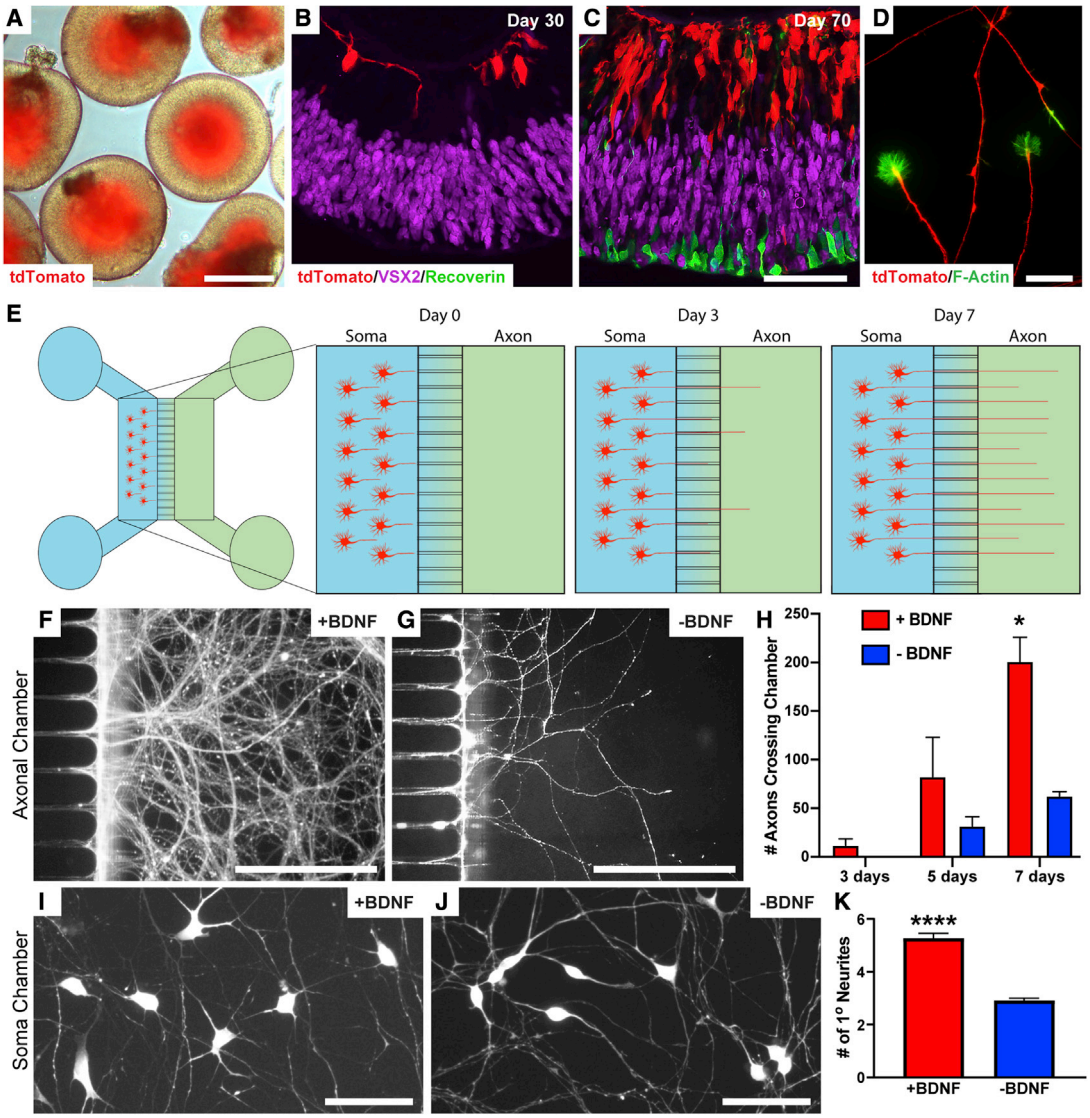

Figure 1. Axonal outgrowth of hPSC-derived RGCs

(A) RGCs were identified within the inner layers of retinal organoids based upon the expression of tdTomato.

(B and C) RGCs develop in the innermost layer of retinal organoids, followed by the development of a distinctly separate photoreceptor layer by 70 days of differentiation. (B) 30 days, (C) 70 days.

(D) Growth cones from developing RGCs were observed at the leading edge of RGC axons.

(E) Schematic of microfluidic platforms for the analysis of RGC axonal outgrowth.

(F–H) Within 1 week, BDNF addition to the axonal chamber significantly increased the recruitment of RGC axons. (F) +BDNF, (G) −BDNF. (H) Number of axons crossing the chamber.

(I–K) More robust outgrowth of RGC axons in response to BDNF treatment was observed by 3 weeks of growth. (I) +BDNF, (J) −BDNF. (K) Number of primary neurites.

Error bars represent SEM, *$p < 0.05$, ****$p < 0.001$. n = 5 separate differentiation experiments each using the H7 line of human embryonic stem cells (hESCs) and the H3 line of human induced pluripotent stem cells (hiPSCs). Scale bars: (A) 400 μm, (B and C) 50 μm, (D) 25 μm, (F and G) 250 μm, (I and J) 30 μm.

retinal and brain organoids were fused together to form assembloids to identify axonal projections from RGCs into a three-dimensional environment mimicking the developing brain (Figures 3C and 3D). Within the first week of growth as assembloids, numerous tdTomato-positive RGC axons extended into brain organoids identified by the expression of the cortical neuronal marker CTIP2 (Figures 3E and 3F). Upon prolonged culture of assembloids, RGC axons grew

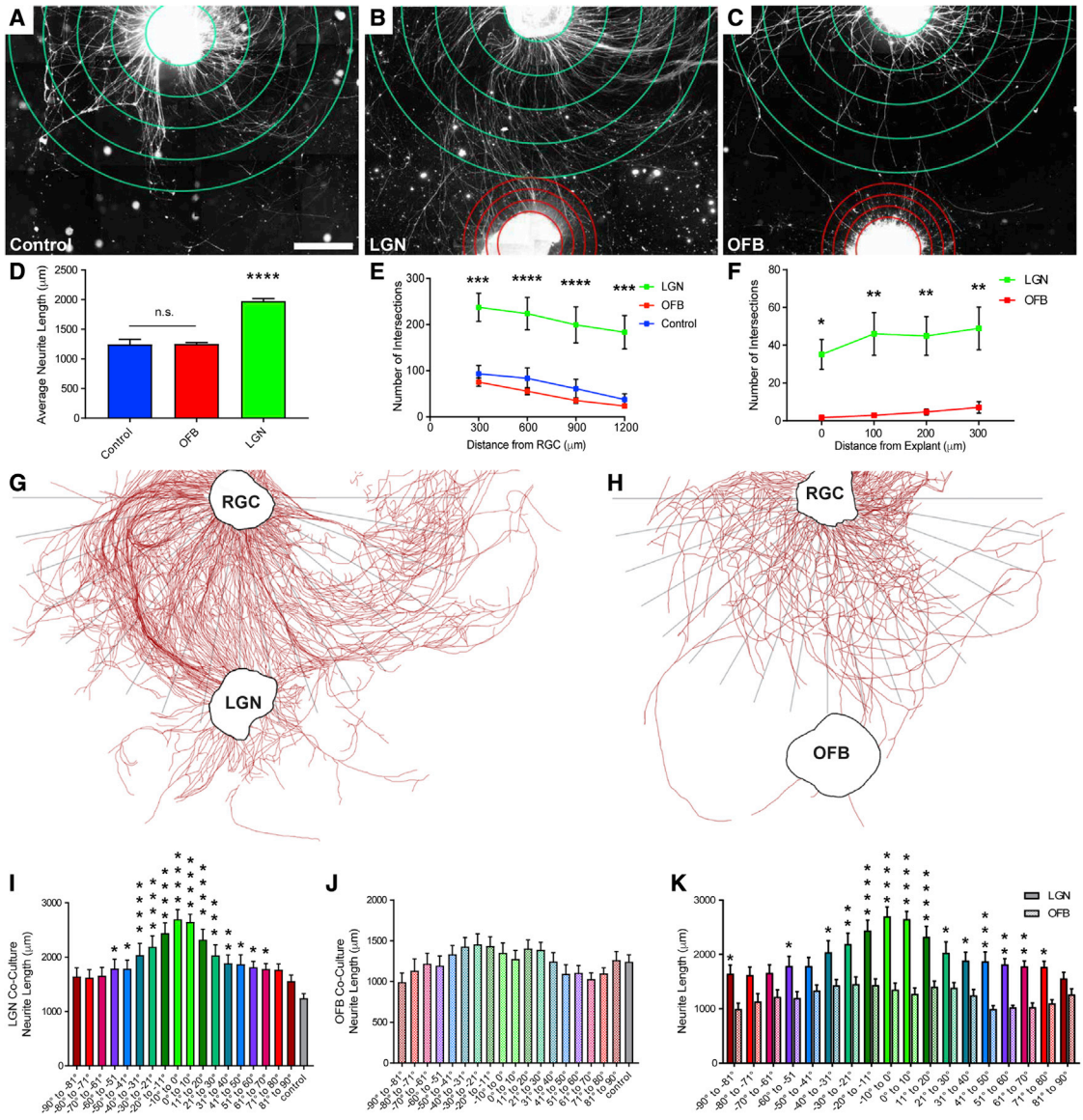

Figure 2. Enhancement of RGC axonal outgrowth in the presence of appropriate post-synaptic target tissue

(A–C) RGC cellular aggregates (top) were grown (A) by themselves or in the presence of explants of either (B) LGN or (C) olfactory bulb tissue (bottom).

(D) Average RGC axon length was significantly increased in the presence of LGN explants.

(E and F) Sholl analyses indicated that significantly more RGC neurites grew in closer proximity to explants compared with olfactory bulb controls. (E) Distance from RGC, (F) distance from explant.

(G and H) Representative tracings demonstrating RGC neurite outgrowth after co-culture with (G) LGN or (H) olfactory bulb. After 1 week in culture the distance of the longest neurite within 10° steps from the explant was measured.

(I and J) Co-culture with (I) LGN explants specifically increased RGC outgrowth compared with (J) controls.

(K) RGC axons that grew closer to LGN explants were significantly longer.

Error bars represent SEM, *$p < 0.05$, **$p < 0.01$, ***$p < 0.005$, ****$p < 0.001$. n = 7 separate differentiation experiments each using the H7 line of hESCs and the H3 line of hiPSCs Scale bar, 500 μm.

longer and more elaborate, reaching deeper into brain organoids with growth-cone-like structures at the leading edge of axons (Figures 3G–3I).

Following the establishment of assembloids (Figure 4A), axonal outgrowth was quantified as the percentage of axons extending into brain organoids based on their

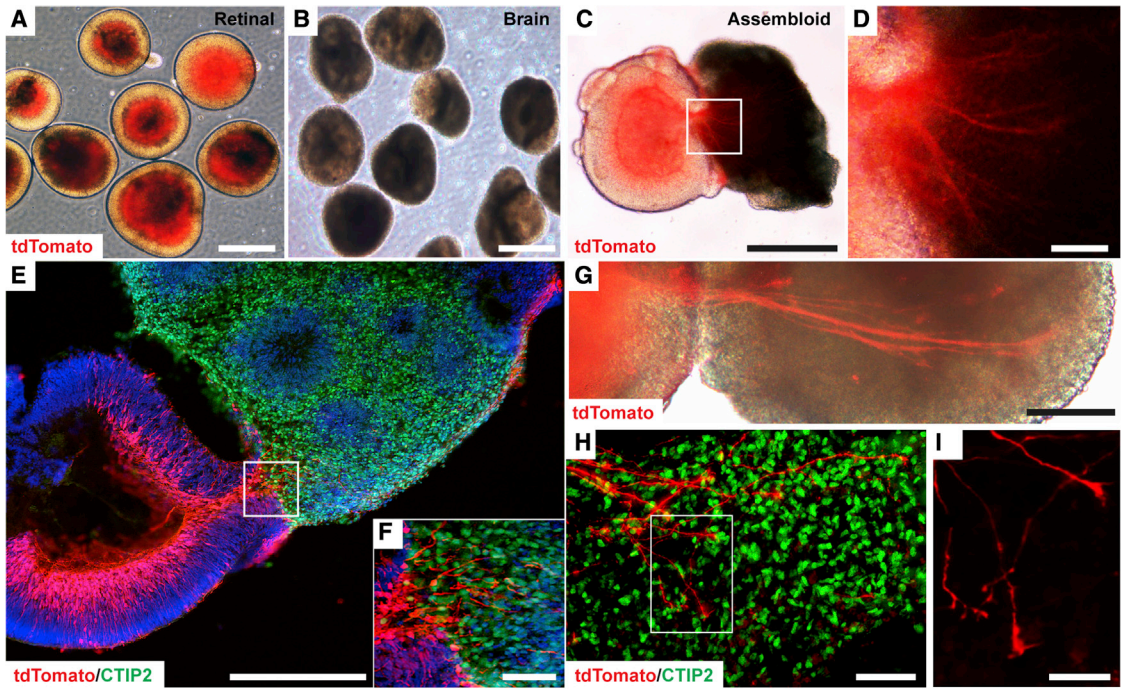

Figure 3. Generation of assembloids from retinal and brain organoids

(A–D) After a total of 50 days of differentiation, retinal organoids and brain organoids were fused together to form assembloids. (A) Retinal, (B) brain, (C) assembloid. (D) Magnified region of box shown in panel C to demonstrate extension of tdTomato-expressing RGC axons into brain organoid.

(E–G) After 1 week, multiple RGC axons extended into CTIP2-positive brain organoids (E and F) and bundled together to form large axonal tracts (G). Box in panel E is magnified in panel F.

(H and I) The active growth of RGC axons was apparent by the presence of growth cone-like structures at the leading edge of RGC axons within brain organoids. Box in panel H is magnified in panel I. n = 6 separate differentiation experiments each using the H7 and H9 lines of hESCs. Scale bars: (A–C) 500 μm, (D) 50 μm, (E) 300 μm, (F) 50 μm, (G) 200 μm, (H) 50 μm, (I) 30 μm.

extension into the beginning (r1), if they reached the middle (r2), or if they reached the distal end (r3) of the brain organoid (Figure 4B), similar to previously described methods (Xiang et al., 2019). RGC axonal extension was quantified from 3 to 7 days post-assembly, in which outgrowth was significantly enhanced into more distal regions of brain organoids (Figures 4C–4E). Interestingly, this axonal outgrowth did not appear to be random, but rather the possibility exists that RGC axons within assembloid models responded to environmental cues, as tdTomato RGC axons were preferentially found within CTIP2-positive neuronal regions rather than SOX2-positive progenitor zones (Figure 4F). Thus, the results of these experiments demonstrated the ability of assembloid models of retinal projections into the brain to serve as effective models of RGC axonal outgrowth and pathfinding.

Assembloid formation results in increased growth and survival of retinal organoids

During retinogenesis, the developing retina receives critical retrograde signaling from targets within the developing brain (Murcia-Belmonte and Erskine, 2019), leading to enhanced survival of retinal neurons including RGCs. While retinal organoid studies to date have closely recapitulated many aspects of retinogenesis (Eldred et al., 2018; Fligor et al., 2018; Wahlin et al., 2017), the isolated growth of retinal organoids in suspension cultures has limited the analysis of these critical interactions between the retina and the brain. The development of assembloids between retinal and brain organoids would thus allow for the analysis of how retrograde signaling modulates the growth and differentiation of developing RGCs. While the maturation of retinal organoids can be a lengthy process extending up to a year in culture, RGCs notoriously do not survive beyond 150 days (Capowski et al., 2019; Wahlin et al., 2017; Zhong et al., 2014), presenting a significant obstacle to the long-term analysis of RGCs in retinal organoids as a developmental or disease-related model. In the current study, retinal organoids within assembloids were significantly larger compared with controls grown alone, almost doubling in size by 150 days of differentiation (Figures 5A–5G). In addition, while a decrease in the number of

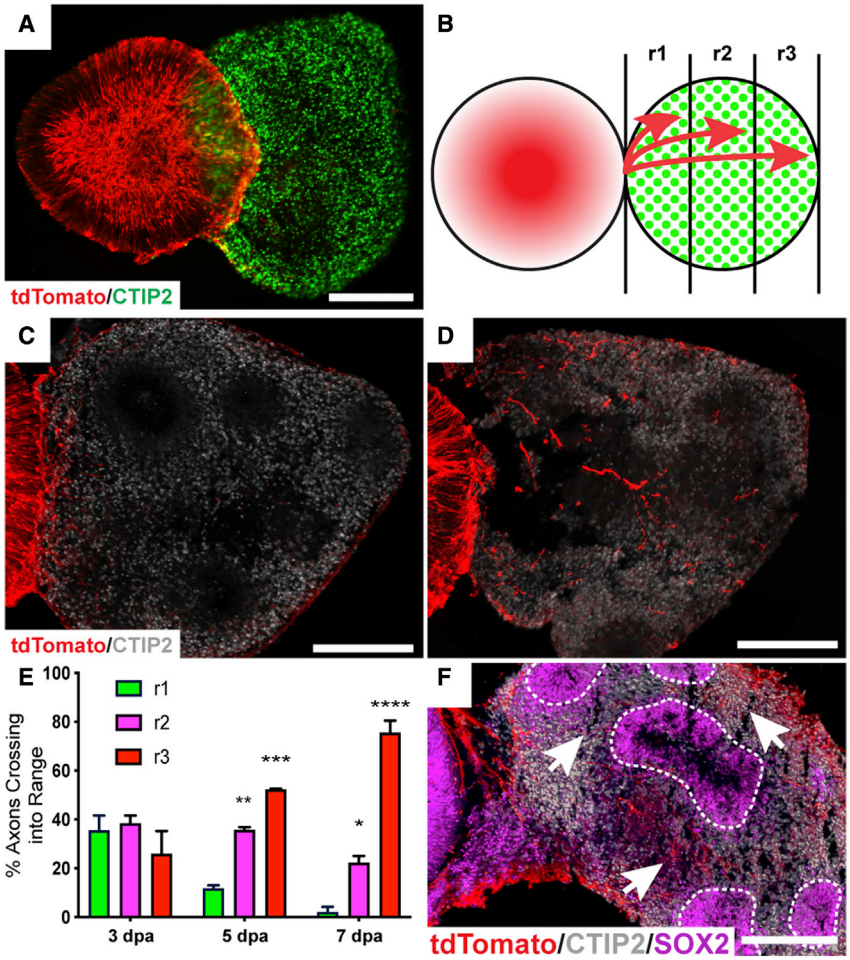

Figure 4. RGC axonal outgrowth and path-finding into assembloids

(A) Retinal organoids expressing POU4F2:tdTomato were fused to CTIP2-positive brain organoids at 50 days of differentiation to analyze the extent of RGC axonal outgrowth into assembloids.

(B) Schematic of the method for quantifying axonal outgrowth from 3 days post-assembly (dpa) to 7 dpa.

(C) By 3 dpa, axons had begun to extend into brain organoids.

(D) More extensive RGC axonal outgrowth was observed by 7 dpa.

(E) By 5 dpa, significantly more axons had reached the midpoint of brain organoids or beyond, with a majority of axons reaching the end of brain organoids by 7 dpa.

(F) RGC axons displayed pathfinding abilities, with more axons (arrows) avoiding SOX2-positive ventricular-like zones (dotted lines), rather than extending through.

Error bars represent SEM, *p < 0.05, **p < 0.01, ***p < 0.005, ****p < 0.001. n = 6 separate differentiation experiments each using the H7 and H9 lines of hESCs. Scale bars, 250 μm.

RGCs was observed in retinal organoids grown alone after 100 days in culture, assembloid cultures supported a continued increase in RGC fluorescence intensity for at least 150 days *in vitro* (Figures 5A–5H).

To explore the possibility that cortical organoids may provide critical growth factors to support this increased size and RGC survival, retinal organoids exhibited significantly increased cell proliferation as well as decreased apoptosis when grown as part of assembloids for 7 days post-assembly, based upon the expression of Ki-67 and active caspase-3, respectively (Figures 5I–5N). To identify candidate factors that could at least partially exert these effects upon retinal organoid growth and confer increased RGC survival, a growth factor array was performed on lysates of brain organoids, which indicated that BDNF was among the most abundant (Figure 5O). To test the ability of BDNF to contribute to retinal organoid growth and RGC survival, individual retinal organoids were treated with exogenous BDNF in the absence of brain organoids at a concentration of 50 ng/mL beginning at day 60 of differentiation (Figures 5P–5S). Under these conditions, more tdTomato-expressing RGCs were observed at 150 days in culture compared with untreated retinal organoids, similar to those levels found within assembloids (Figure 5T), although the overall size of retinal organoids remained unchanged compared with untreated controls (Figure 5U).

Reconstructing retinotectal projections with retinal, thalamic, and cortical organoids

Within the brain, the major post-synaptic targets for RGCs are found within the thalamus, particularly the LGN as well as the superior colliculus as primary targets (Murcia-Belmonte and Erskine, 2019). Given the highly specialized and diverse functions of different brain regions, as well as differences in the signals they can produce for growing axons, the ability to more effectively model connections between the retina and the thalamus using hPSC-derived organoids would offer numerous opportunities for the study of the human visual pathway. As such, given the recent derivation of thalamic organoids from hPSCs (Xiang

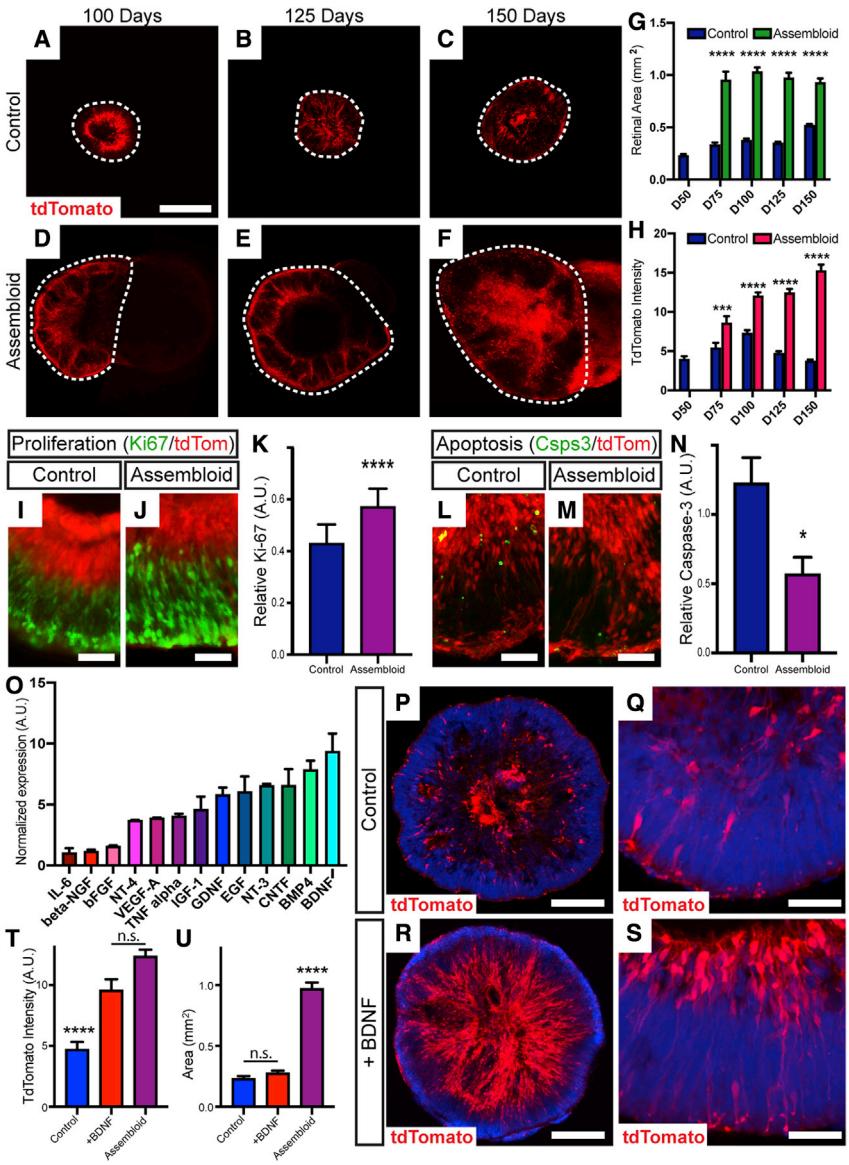

Figure 5. Long-term maintenance of RGCs in retinal organoids

(A–F) Retinal organoids were maintained up to 150 days in culture (A–C) and compared with age-matched retinocortical assembloids (D–F). Area of retinal organoid indicated by dashed line.

(G) Retinal area was significantly increased in assembloids.

(H) POU4F2:tdTomato expression began to decrease in control organoids after 100 days in culture, while expression was significantly increased in assembloids.

(I–K) Assembloids displayed significantly increased cell proliferation indicated by Ki67 immunoreactivity compared with age-matched controls. (I) Control, (J) assembloid, (K) relative Ki-67.

(L–N) Concurrently, a significant decrease in the expression of active caspase-3 within retinal regions was observed. (L) Control, (M) assembloid, (N) relative caspase-3.

(O) Cytokine array analysis of brain organoid lysates, with BDNF identified as the most highly expressed.

(P–U) Exogenous BDNF resulted in enhanced organization and increased POU4F2:tdTomato expression in long-term cultures, while no significant difference was observed in the size of retinal organoids. (P, Q) Control, (R, S) +BDNF, (T) tdTomato intensity, (U) area.

Error bars represent SEM, *$p < 0.05$, ***$p < 0.005$, ****$p < 0.001$. n = 5 separate differentiation experiments each using the H7 and H9 lines of hESCs. Scale bars: (A–F) 500 μm, (I, J, L, and M) 50 μm, (P and R) 200 μm, (Q and S) 50 μm.

et al., 2019), efforts were undertaken to more specifically model projections of the visual pathway with assembloids generated from retinal, thalamic, and cortical organoids.

To construct an assembloid model of the visual pathway, thalamic and cortical organoids were differentiated following established methods (Figures S2 and S3), and assembloids were then configured to join retinal, thalamic, and cortical organoids in order (Figure 6A). To aid in identification of cells originating from each organoid, particularly long-distance axonal projections from one organoid to another, retinal organoids were generated from hPSCs with a POU4F2:tdTomato reporter, while thalamic organoids were generated with a GFP reporter (Figures 6B and 6C). Assembloids were then generated after 50 total days of differentiation, and cells from each organoid could be readily identified by the expression of fluorescent proteins or through immunostaining of cortical organoids for the robust expression of CTIP2 (Figure 6C).

Within 1 week following the fusion of organoids to form assembloids, tdTomato-expressing RGC axons robustly extended into GFP-expressing thalamic organoids (Figures 6D–6F). Interestingly, while RGC axons extending into thalamic organoids appeared shorter than those that previously extended into brain organoids (Figure 4D), significantly greater numbers of RGC axons extended into thalamic organoids (Figure 6G), suggesting differences in the environments between thalamic and prosencephalic brain organoids affecting RGC axonal outgrowth. In

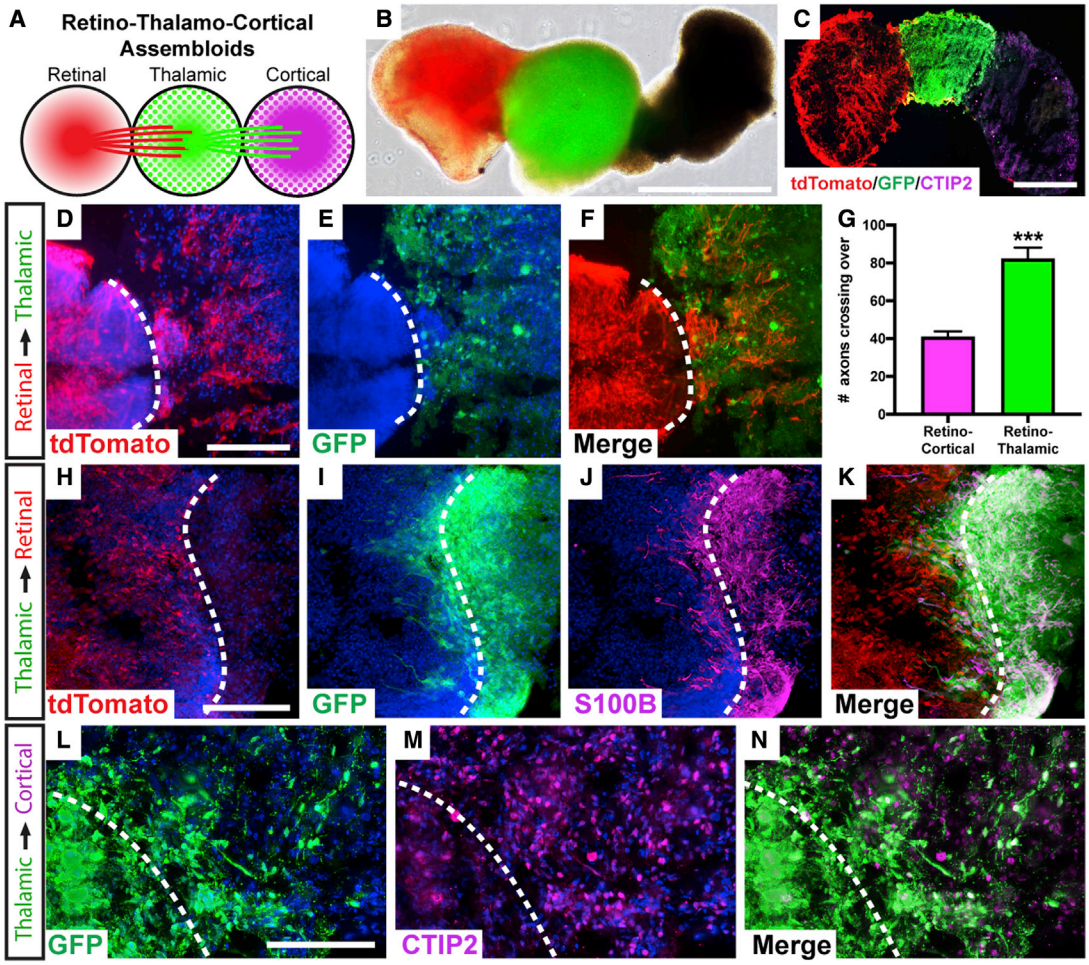

Figure 6. Visual pathway reconstruction with retinal, thalamic, and cortical organoids

(A) Schematic of strategy to generate tri-assembloids from retinal, thalamic, and cortical organoids.

(B and C) (B) Fluorescent reporters were used to identify various organoids and their projections, with retinal organoids expressing a POU4F2:tdTomato reporter and thalamic organoids expressing a GFP reporter. (C) Staining of cortical organoids with CTIP2 verified their identity.

(D–F) Following the formation of assembloids, tdTomato-expressing RGC axons robustly extended into GFP-expressing thalamic organoids. (D) tdTomato, (E) GFP, (F) merge.

(G) Significantly greater numbers of RGC axons had extended into thalamic organoids compared with brain organoids at the same time point.

(H–K) After an additional 2 months, GFP-expressing thalamic cells migrated retrogradely into retinal organoids, with these migratory cells expressing the early astrocyte marker S100β. (H) tdTomato, (I) GFP, (J) S100β, (K) merge.

(L–N) Between thalamic and cortical organoids, robust extension of GFP-expressing neurites was observed entering CTIP2-positive cortical organoids. (L) GFP, (M) CTIP2, (N) merge

Error bars represent SEM, ***$p < 0.005$. n = 6 separate differentiation experiments each using the H7 and H9 lines of hESCs and the tiPS5 line of hiPSCs. Scale bars: (B) 800 μm, (C) 400 μm, (D–F) 200 μm, (H–K) 150 μm, (L–N) 150 μm. Dashed line indicates boundary between different organoids within assembloid, as indicated on the left margin.

addition, while RGC axons robustly extended into thalamic organoids, no evidence was observed for GFP-positive thalamic cells extending into retinal organoids at early time points, demonstrating a largely unidirectional path of axonal outgrowth. Within an additional 2 months, GFP-expressing thalamic cells began migrating retrogradely into retinal organoids. Interestingly, these migratory cells were mostly S100β-expressing astrocytes (Figures 6H–6K), somewhat reminiscent of the migration of astrocytes during neural development into the retina. Conversely, robust extension of GFP-expressing neurites was observed entering cortical organoids (Figures 6L–6N), similar to the outgrowth of thalamic neurons toward the visual cortex. Overall, the use of retinal, thalamic, and cortical organoids

to form assembloids allowed for the *in vitro* modeling of several aspects of the development of the visual pathway.

DISCUSSION

The results presented here demonstrate the establishment of novel approaches for the study of human RGC axonal outgrowth and pathfinding, including the response of RGC axons to extrinsic factors as well as the ability of hPSC-derived RGCs to navigate through neural environments to reach post-synaptic targets. The establishment of three-dimensional assembloids from retinal, thalamic, and cortical organoids provided a more physiologically relevant model of the visual pathway, facilitating the exploration of how axons navigate the neural environment to reach post-synaptic targets as well as how connections are established in this pathway in a novel human cellular *in vitro* system.

In the current study, RGC axons were effectively recruited in response to a gradient of signaling factors, particularly BDNF, as a retrograde signaling factor that is known to be provided to RGCs from targets within the brain (Pease et al., 2000; Quigley et al., 2000). Interestingly, explants of mouse LGN influenced not only the length of RGC axonal outgrowth, but also the directionality of outgrowth, as RGCs preferentially extended toward LGN explants, whereas similar experiments using olfactory bulb explants failed to recapitulate these effects. As axonal outgrowth and pathfinding are dynamic processes, with axonal growth cones regularly extending and retracting in response to environmental cues, the cause of increased RGC axonal outgrowth in the presence of LGN explants could be due to a variety of factors. It is possible that LGN explant tissue released a more suitable cocktail of growth factors to recruit RGC axons. Alternatively, it is possible that the process of axonal outgrowth itself was not particularly affected, but rather, the LGN explant may have served as a desirable target for RGC axons that limited subsequent retraction, essentially locking these axons in place and enhancing their total length and number. In future studies, it will be interesting to identify factors differentially produced from post-synaptic targets that serve as attractive cues for developing RGC axons.

While organoid models provide a strong *in vitro* platform for studies of cell fate determination and organization, they are typically limited to a particular tissue type and, thus, limited in their ability to effectively model the long-distance axonal extensions of RGCs and other projection neurons of the nervous system. A number of previous studies have demonstrated the ability of retinal organoids to give rise to RGCs in a spatiotemporally appropriate manner, yet these cells are often lost by later stages of differentiation (Capowski et al., 2019; Sridhar et al., 2020; Zhong et al., 2014). While a variety of possibilities may explain this phenomenon, the "neurotrophic hypothesis" may be a likely cause, meaning that those RGCs that receive retrograde neurotrophic factors will survive, while those that lack retrograde survival support will undergo apoptosis (Northcutt, 1989; von Bartheld et al., 1996).

To address the shortcomings of retinal organoids for the long-term study of RGCs and their axonal projections, the current study focused on the development of three-dimensional assembloid models of the visual system not only to enhance the viability of hPSC-derived RGCs, but also to provide a more physiologically relevant environment for the growth of RGC axons. The concept of three-dimensional assembloid models has been recently described (Amin and Pașca, 2018), and in it regionally patterned cells and/or organoids are combined to more effectively model interactions between different cell types, particularly those from different brain regions. Results from the current study demonstrated a robust extension of RGC axons into assembloid models, with RGC axons demonstrating the recognition of environmental cues to guide their outgrowth. Interestingly, these axons often avoided regions of neural rosettes within brain organoids, resembling ventricular zones of the developing brain, similar to previous studies that have demonstrated chemorepulsive cues provided by ventricular zones in the brain that function to guide the direction of neuronal migration and axonal pathfinding (Andrews et al., 2007; Yeh et al., 2014). In addition, while RGC axons were capable of growth into varied assembloid models, RGCs extended longer axons into prosencephalic brain organoids, yet the number of RGC axons was increased within thalamic organoids. These observations suggest that the environment within thalamic organoids provides more suitable cues for RGCs to explore rather than quickly pass through, reminiscent of topographic mapping in the tectum when RGCs begin to enter the LGN and slow their growth and increase branching in the stages prior to refinement (Dingwell et al., 2000; Godement and Mason, 1993). Overall, these results will provide a foundation for future studies of human RGC axonal outgrowth and the environmental cues that guide this pathfinding.

The study of retinal organoids in recent years has provided tremendous insight into mechanisms underlying the specification of the human retina (Capowski et al., 2019; Cowan et al., 2020; Sridhar et al., 2020), with a particular focus upon photoreceptor development and organization (Eldred et al., 2018; Kallman et al., 2020; Wahlin et al., 2017). However, a number of shortcomings of retinal organoids remain, including the eventual loss of RGCs from retinal organoids in long-term cultures as well as the inability of retinal organoids to approximate the size of

the developing human retina. The current study demonstrated a significantly increased survival of RGCs within assembloids compared with those RGCs grown within retinal organoids lacking access to downstream targets. In further support of the neurotrophic hypothesis (Northcutt, 1989; von Bartheld et al., 1996), BDNF was identified as a leading growth factor produced by brain organoids, and further supplementation of retinal organoids with exogenous BDNF resulted in the enhanced survival of RGCs in long-term cultures. In addition, increased survival of RGCs in assembloids was associated with an increased size of the retinal organoid component of assembloids due to a combination of both increased cell proliferation and decreased apoptosis. Interestingly, while exogenous BDNF exposure led to increased RGC survival, it was insufficient to confer an increased size of retinal organoids as observed in assembloid cultures, suggesting other factors are likely involved in observed size differences. In future studies, it will be important to determine the degree to which other brain-derived factors play a role in the survival and growth of retinal organoids, as previous studies have demonstrated that a variety of growth factors play a role in RGC survival, axonal outgrowth, and regeneration (Goldberg et al., 2002; Meyer-Franke et al., 1995).

Within the mammalian retina, numerous subtypes of RGCs exist, with diversity based on morphology, transcriptional profile, and function (Laboissonniere et al., 2019; Rheaume et al., 2018). In addition, numerous reports have detailed the selective susceptibility of certain RGC subtypes in disease states such as glaucoma (Della Santina et al., 2013; Ou et al., 2016; Tran et al., 2019; VanderWall et al., 2020b). Given the ability to enhance overall RGC survival within retinal organoids and assembloids, it may also be possible to study the differential susceptibility of RGC subtypes in future studies. Similarly, it is also important to note that the use of the POU4F2:tdTomato:Thy1.2 reporter line in this study is an efficient method for RGC identification and purification, yet this purification selects for RGCs that express POU4F2. While POU4F2 is expressed by a large majority of RGCs in the retina (Xiang et al., 1997), it is important to note that these RGCs may not accurately represent the entire population of RGCs found in organoids.

In long-term cultures, thalamic organoid-derived S100β-positive cells appeared to migrate into retinal organoids, coinciding with the crucial time point at which RGC populations typically declined (Capowski et al., 2019; Sridhar et al., 2020; Zhong et al., 2014). A decline in RGC populations is most likely the result of a combination of factors, particularly a lack of important support cells such as astrocytes. *In vivo*, astrocytes can be found along the nerve fiber layer of the retina as well as throughout the optic nerve (Chu et al., 2001; Tao and Zhang, 2014). Therefore, the increased survival of RGC populations within assembloids may be a result of the introduction of crucial supporting glial cells that are not native to retinal organoids. Moreover, cell migration was also observed from the thalamus into cortical organoids, reminiscent of thalamic projections that relay information from the LGN to the primary visual cortex. Therefore, the assembly of retinal-thalamic-cortical tri-assembloids begins to mimic the early stages of visual circuit formation.

The ability to more closely recapitulate the extracellular environment surrounding RGC axons through the use of assembloids will also have important implications for the study of neurodegenerative diseases such as glaucoma. RGCs are highly compartmentalized neurons, with neurodegeneration in glaucoma occurring via distinct mechanisms in the axon compared with the cell body and dendrites (Syc-Mazurek and Libby, 2019; Whitmore et al., 2005). Correspondingly, the initial insult to RGCs in glaucoma occurs within the axonal compartment when axons leave the eye through the optic nerve head. While previous studies have been able to study some features of glaucomatous neurodegeneration with retinal organoids (VanderWall et al., 2020a), the ability to study neurodegenerative features associated with RGC compartmentalization has not been previously possible. Through the use of assembloid models, future studies of glaucomatous neurodegeneration can be greatly facilitated in a manner that can be adapted to more accurately reflect the extracellular environment and how these factors modulate the disease phenotype, particularly factors that contribute in a non-cell-autonomous manner.

While the current study demonstrates the feasibility of establishing retinal-thalamic-cortical assembloids with hPSC-derived organoid models, in the future it will be important to refine these strategies to better reflect the spatial organization of these brain regions. The ability to utilize assembloid models remains limited by inadequate organization of many organoid models (Del Dosso et al., 2020). Further refinements in the differentiation of organoids in the future will contribute to refinements in the composition and organization of assembloids and will aid in the application of assembloids for studies of the development of the visual pathway as well as how this pathway is adversely affected in disease states. It will also be of interest to investigate whether assembloid models can be adapted to examine the formation of functional synaptic contacts between different brain regions, including whether assembloids can demonstrate functional responses to light stimuli along the complete visual pathway.

Overall, the development of retinal-thalamic-cortical assembloids serves as an effective *in vitro* model of the long-distance projections between the retina and the brain, with RGC axons significantly extending into assembloids

and thalamic neurons similarly extending into cortical regions. Furthermore, by providing an appropriate environment for RGCs to extend their axons, the growth of retinal organoids as a whole was enhanced, including a significant increase in RGC survival. As such, these results will facilitate the use of assembloids for disease modeling and pharmaceutical screening, as well as providing a model for studies of RGC axonal outgrowth and regeneration.

EXPERIMENTAL PROCEDURES

Differentiation of regional organoids

hPSCs were expanded and passaged as previously described (Meyer et al., 2009). For retinal organoids, hPSCs were differentiated following previously established protocols (Fligor et al., 2020; Sridhar et al., 2016). Prosencephalic brain organoids were differentiated from hPSCs through similar methods (Fligor et al., 2020; Meyer et al., 2011; Ohlemacher et al., 2015), as brain organoids have been previously demonstrated to be derived in parallel with retinal organoids. Briefly, BMP4 was excluded from the medium at day 6 of differentiation and embryoid bodies were plated on laminin-coated plates 2 days later, with all subsequent conditions maintained the same. Thalamic organoids were differentiated following a previously published protocol (Xiang et al., 2019). Experimental details for differentiation of organoids are provided in the supplemental experimental procedures. All experiments were performed following approval by the Indiana University Institutional Biosafety Committee.

Growth of hPSC-derived RGCs in microfluidic platforms

RGCs were purified from retinal organoids as previously described (Sluch et al., 2017; VanderWall et al., 2020a) and subsequently seeded into microfluidic devices (Xona Microfluidics, XC450). Axons were recruited to cross into the contralateral chamber through the establishment of a volume differential as well as a gradient of BDNF. Experimental details for growth in microfluidic devices are provided in the supplemental experimental procedures.

Co-culture of RGCs and mouse brain explants

Mouse LGN tissue was harvested from P0–P2 neonatal mice following protocols approved by the Institutional Animal Care and Use Committee within the School of Science at Indiana University Purdue University Indianapolis and were conducted in accordance with the ARVO *Statement for the Use of Animals in Ophthalmic and Vision Research*. To establish co-cultures between mouse LGN explants and hPSC-derived RGCs, cell aggregates and explants were cultured in a two-chambered silicone culture insert (Ibidi), and this insert was removed after cultures were established to analyze cellular interactions and axonal outgrowth. Experimental details for co-cultures are provided in the supplemental experimental procedures.

Establishment of assembloid cultures

Regionally specified organoids were initially differentiated as described above and induced to fuse together at 50 days of differentiation to generate assembloids following protocols established for other systems (Sloan et al., 2018). Briefly, to generate assembloids between retinal and prosencephalic brain organoids, a single POU4F2:tdTomato-positive retinal organoid was fused with a single brain organoid by placing each into a single 1.5 mL centrifuge tube and incubating at 37°C at 5% CO_2 to allow the organoids to fuse together. Three days later, fused assembloids were transferred to a single well of a low-attachment 24-well plate (Corning) for further maturation in RDM supplemented with 10% FBS, 1× Glutamax, and 100 μM taurine, with the medium changed every 2–3 days. Tri-assembloids with retinal, thalamic, and cortical organoids were established upon membranes to allow for more controlled positioning of organoids. Three days after assembly, tri-assembloids were transferred into individual wells of a low-attachment 24-well plate and maintained as outlined above. At indicated time points, assembloids were collected and fixed in 4% paraformaldehyde before cryostat sectioning for immunocytochemical analyses.

Immunocytochemistry and microscopy

Immunostaining was performed as previously described, with the antibodies used detailed in Table S1. Microscopy was performed on a Leica 5500DM fluorescence microscope with images captured by a Hamamatsu Orca-R2 digital camera using the Leica Application Suite software. Details for immunocytochemistry are provided in the supplemental experimental procedures.

Growth factor array

Growth factor array analysis was performed using the C-Series Human Cytokine Antibody Array C1000 (RayBiotech no. AAh-CYT-1000-2) following the manufacturer's instructions. Blots were imaged using a chemiluminescence imaging system (Odyssey CLX, LiCor) and analyzed using the gel analysis function in ImageJ. Experimental details are provided in the supplemental experimental procedures.

Data quantification and statistical analyses

For quantification of experimental results, as well as determination of statistically significant differences, data were collected and analyzed in GraphPad Prism software. Details about data quantification and statistical analyses are provided in the supplemental experimental procedures.

SUPPLEMENTAL INFORMATION

Supplemental information can be found online at https://doi.org/10.1016/j.stemcr.2021.05.009.

AUTHOR CONTRIBUTIONS

C.M.F. designed experiments, collected and analyzed data, and co-wrote the manuscript. S.S.L., J.H., P.K.S., K.B.V., and K.C.H. collected and analyzed data. C.G. collected and analyzed data and edited the manuscript. J.S.M. designed experiments, analyzed data, co-wrote the manuscript, and gave final approval of the manuscript.

CONFLICTS OF INTEREST

The authors declare no competing interests.

ACKNOWLEDGMENTS

We thank William Guido and Guela Sokhadze for assistance with the isolation of mouse LGN explants for *in vitro* cultures, and Don Zack and Valentin Sluch for the POU4F2:tdTomato cell line. This work was supported by the National Eye Institute (R01 EY024984 and R21 EY031120 to J.S.M.), the BrightFocus Foundation (G2020369 to J.S.M.), and the Indiana Department of Health Spinal Cord and Brain Injury Research Fund (26343 to J.S.M.). This publication was also made possible by an Indiana CTSI predoctoral research fellowship (UL1TR002529, A. Shekhar, PI) from the National Institutes of Health, National Center for Advancing Translational Sciences, Clinical and Translational Sciences Award (K.B.V.).

Received: January 29, 2021
Revised: May 12, 2021
Accepted: May 13, 2021
Published: June 10, 2021

REFERENCES

Ader, M., and Tanaka, E.M. (2014). Modeling human development in 3D culture. Curr. Opin. Cell Biol. *31*, 23–28.

Amin, N.D., and Paşca, S.P. (2018). Building models of brain disorders with three-dimensional organoids. Neuron *100*, 389–405.

Andrews, W.D., Barber, M., and Parnavelas, J.G. (2007). Slit-Robo interactions during cortical development. J. Anat. *211*, 188–198.

Brown, J., Quadrato, G., and Arlotta, P. (2018). Studying the brain in a dish: 3D cell culture models of human brain development and disease. Curr. Top. Dev. Biol. *129*, 99–122.

Capowski, E.E., Samimi, K., Mayerl, S.J., Phillips, M.J., Pinilla, I., Howden, S.E., Saha, J., Jansen, A.D., Edwards, K.L., Jager, L.D., et al. (2019). Reproducibility and staging of 3D human retinal organoids across multiple pluripotent stem cell lines. Development *146*, dev171686.

Chen, A., Guo, Z., Fang, L., and Bian, S. (2020). Application of fused organoid models to study human brain development and neural disorders. Front. Cell. Neurosci. *14*, 133.

Chu, Y., Hughes, S., and Chan-Ling, T. (2001). Differentiation and migration of astrocyte precursor cells and astrocytes in human fetal retina: relevance to optic nerve coloboma. FASEB J. *15*, 2013–2015.

Cowan, C.S., Renner, M., De Gennaro, M., Gross-Scherf, B., Goldblum, D., Hou, Y., Munz, M., Rodrigues, T.M., Krol, J., Szikra, T., et al. (2020). Cell types of the human retina and its organoids at single-cell resolution. Cell *182*, 1623–1640.e1634.

Crair, M.C., and Mason, C.A. (2016). Reconnecting eye to brain. J. Neurosci. *36*, 10707–10722.

Del Dosso, A., Urenda, J.P., Nguyen, T., and Quadrato, G. (2020). Upgrading the physiological relevance of human brain organoids. Neuron *107*, 1014–1028.

Della Santina, L., Inman, D.M., Lupien, C.B., Horner, P.J., and Wong, R.O. (2013). Differential progression of structural and functional alterations in distinct retinal ganglion cell types in a mouse model of glaucoma. J. Neurosci. *33*, 17444–17457.

Dingwell, K.S., Holt, C.E., and Harris, W.A. (2000). The multiple decisions made by growth cones of RGCs as they navigate from the retina to the tectum in Xenopus embryos. J. Neurobiol. *44*, 246–259.

Eldred, K.C., Hadyniak, S.E., Hussey, K.A., Brenerman, B., Zhang, P.W., Chamling, X., Sluch, V.M., Welsbie, D.S., Hattar, S., Taylor, J., et al. (2018). Thyroid hormone signaling specifies cone subtypes in human retinal organoids. Science *362*, eaau6348.

Fligor, C.M., Huang, K.C., Lavekar, S.S., VanderWall, K.B., and Meyer, J.S. (2020). Differentiation of retinal organoids from human pluripotent stem cells. Methods Cell Biol. *159*, 279–302.

Fligor, C.M., Langer, K.B., Sridhar, A., Ren, Y., Shields, P.K., Edler, M.C., Ohlemacher, S.K., Sluch, V.M., Zack, D.J., Zhang, C., et al. (2018). Three-dimensional retinal organoids facilitate the investigation of retinal ganglion cell development, organization and neurite outgrowth from human pluripotent stem cells. Sci. Rep. *8*, 14520.

Godement, P., and Mason, C.A. (1993). Guidance of retinal fibers in the optic chiasm. Perspect. Dev. Neurobiol. *1*, 217–225.

Goldberg, J.L., Espinosa, J.S., Xu, Y., Davidson, N., Kovacs, G.T., and Barres, B.A. (2002). Retinal ganglion cells do not extend axons by default: promotion by neurotrophic signaling and electrical activity. Neuron *33*, 689–702.

Huang, K.C., Wang, M.L., Chen, S.J., Kuo, J.C., Wang, W.J., Nhi Nguyen, P.N., Wahlin, K.J., Lu, J.F., Tran, A.A., Shi, M., et al. (2019). Morphological and molecular defects in human three-dimensional retinal organoid model of X-linked juvenile retinoschisis. Stem Cell Rep. *13*, 906–923.

Kallman, A., Capowski, E.E., Wang, J., Kaushik, A.M., Jansen, A.D., Edwards, K.L., Chen, L., Berlinicke, C.A., Joseph Phillips, M., Pierce, E.A., et al. (2020). Investigating cone photoreceptor development using patient-derived NRL null retinal organoids. Commun. Biol. *3*, 82.

Laboissonniere, L.A., Goetz, J.J., Martin, G.M., Bi, R., Lund, T.J.S., Ellson, L., Lynch, M.R., Mooney, B., Wickham, H., Liu, P., et al. (2019). Molecular signatures of retinal ganglion cells revealed through single cell profiling. Sci. Rep. *9*, 15778.

Lancaster, M.A., and Knoblich, J.A. (2014). Organogenesis in a dish: modeling development and disease using organoid technologies. Science *345*, 1247125.

Lane, A., Jovanovic, K., Shortall, C., Ottaviani, D., Panes, A.B., Schwarz, N., Guarascio, R., Hayes, M.J., Palfi, A., Chadderton, N., et al. (2020). Modeling and rescue of RP2 retinitis pigmentosa using iPSC-derived retinal organoids. Stem Cell Rep. *15*, 67–79.

Lu, A.Q., and Barnstable, C.J. (2019). Pluripotent stem cells as models of retina development. Mol. Neurobiol. *56*, 6056–6070.

Meyer, J.S., Howden, S.E., Wallace, K.A., Verhoeven, A.D., Wright, L.S., Capowski, E.E., Pinilla, I., Martin, J.M., Tian, S., Stewart, R., et al. (2011). Optic vesicle-like structures derived from human pluripotent stem cells facilitate a customized approach to retinal disease treatment. Stem Cells *29*, 1206–1218.

Meyer, J.S., Shearer, R.L., Capowski, E.E., Wright, L.S., Wallace, K.A., McMillan, E.L., Zhang, S.C., and Gamm, D.M. (2009). Modeling early retinal development with human embryonic and

induced pluripotent stem cells. Proc. Natl. Acad. Sci. U S A *106*, 16698–16703.

Meyer-Franke, A., Kaplan, M.R., Pfrieger, F.W., and Barres, B.A. (1995). Characterization of the signaling interactions that promote the survival and growth of developing retinal ganglion cells in culture. Neuron *15*, 805–819.

Miura, Y., Li, M.Y., Birey, F., Ikeda, K., Revah, O., Thete, M.V., Park, J.Y., Puno, A., Lee, S.H., Porteus, M.H., et al. (2020). Generation of human striatal organoids and cortico-striatal assembloids from human pluripotent stem cells. Nat. Biotechnol. *38*, 1421–1430.

Murcia-Belmonte, V., and Erskine, L. (2019). Wiring the binocular visual pathways. Int. J. Mol. Sci. *20*, 3282.

Northcutt, R.G. (1989). Body and Brain. A Trophic Theory of Neural Connections. Dale Purves. Harvard University Press, Cambridge, MA, 1988. , 231 pp., illus. $35. Science *244*, 993.

Ohlemacher, S.K., Iglesias, C.L., Sridhar, A., Gamm, D.M., and Meyer, J.S. (2015). Generation of highly enriched populations of optic vesicle-like retinal cells from human pluripotent stem cells. Curr. Protoc. Stem Cell Biol. *32*, 1h.8.1–1h.8.20.

Ou, Y., Jo, R.E., Ullian, E.M., Wong, R.O., and Della Santina, L. (2016). Selective vulnerability of specific retinal ganglion cell types and synapses after transient ocular hypertension. J. Neurosci. *36*, 9240–9252.

Parfitt, D.A., Lane, A., Ramsden, C.M., Carr, A.F., Munro, P.M., Jovanovic, K., Schwarz, N., Kanuga, N., Muthiah, M.N., Hull, S., et al. (2016). Identification and correction of mechanisms underlying inherited blindness in human iPSC-derived optic cups. Cell Stem Cell *18*, 769–781.

Pease, M.E., McKinnon, S.J., Quigley, H.A., Kerrigan-Baumrind, L.A., and Zack, D.J. (2000). Obstructed axonal transport of BDNF and its receptor TrkB in experimental glaucoma. Invest. Ophthalmol. Vis. Sci. *41*, 764–774.

Quadrato, G., and Arlotta, P. (2017). Present and future of modeling human brain development in 3D organoids. Curr. Opin. Cell Biol *49*, 47–52.

Quigley, H.A., McKinnon, S.J., Zack, D.J., Pease, M.E., Kerrigan-Baumrind, L.A., Kerrigan, D.F., and Mitchell, R.S. (2000). Retrograde axonal transport of BDNF in retinal ganglion cells is blocked by acute IOP elevation in rats. Invest. Ophthalmol. Vis. Sci. *41*, 3460–3466.

Rheaume, B.A., Jereen, A., Bolisetty, M., Sajid, M.S., Yang, Y., Renna, K., Sun, L., Robson, P., and Trakhtenberg, E.F. (2018). Single cell transcriptome profiling of retinal ganglion cells identifies cellular subtypes. Nat. Commun. *9*, 2759.

Sloan, S.A., Andersen, J., Paşca, A.M., Birey, F., and Paşca, S.P. (2018). Generation and assembly of human brain region-specific three-dimensional cultures. Nat. Protoc. *13*, 2062–2085.

Sluch, V.M., Chamling, X., Liu, M.M., Berlinicke, C.A., Cheng, J., Mitchell, K.L., Welsbie, D.S., and Zack, D.J. (2017). Enhanced stem cell differentiation and immunopurification of genome engineered human retinal ganglion cells. Stem Cells Transl. Med. *6*, 1972–1986.

Sridhar, A., Hoshino, A., Finkbeiner, C.R., Chitsazan, A., Dai, L., Haugan, A.K., Eschenbacher, K.M., Jackson, D.L., Trapnell, C., Bermingham-McDonogh, O., et al. (2020). Single-cell transcriptomic comparison of human fetal retina, hPSC-derived retinal organoids, and long-term retinal cultures. Cell Rep. *30*, 1644–1659.e1644.

Sridhar, A., Langer, K.B., Fligor, C.M., Steinhart, M., Miller, C.A., Ho-A-Lim, K.T., Ohlemacher, S.K., and Meyer, J.S. (2018). Human pluirpotent stem cells as in vitro models for retinal development and disease. In Regenerative Medicine and Stem Cell Therapy for the Eye, B. Ballios and M.J. Young, eds. (Springer Nature), pp. 17–49.

Sridhar, A., Ohlemacher, S.K., Langer, K.B., and Meyer, J.S. (2016). Robust differentiation of mRNA-reprogrammed human induced pluripotent stem cells toward a retinal lineage. Stem Cells Transl. Med. *5*, 417–426.

Sridhar, A., Steward, M.M., and Meyer, J.S. (2013). Nonxenogeneic growth and retinal differentiation of human induced pluripotent stem cells. Stem Cells Transl. Med. *2*, 255–264.

Syc-Mazurek, S.B., and Libby, R.T. (2019). Axon injury signaling and compartmentalized injury response in glaucoma. Prog. Retin. Eye Res. *73*, 100769.

Tao, C., and Zhang, X. (2014). Development of astrocytes in the vertebrate eye. Dev. Dyn. *243*, 1501–1510.

Tran, N.M., Shekhar, K., Whitney, I.E., Jacobi, A., Benhar, I., Hong, G., Yan, W., Adiconis, X., Arnold, M.E., Lee, J.M., et al. (2019). Single-cell profiles of retinal ganglion cells differing in resilience to injury reveal neuroprotective genes. Neuron *104*, 1039–1055.e1012.

VanderWall, K.B., Huang, K.C., Pan, Y., Lavekar, S.S., Fligor, C.M., Allsop, A.R., Lentsch, K.A., Dang, P., Zhang, C., Tseng, H.C., et al. (2020a). Retinal ganglion cells with a glaucoma OPTN(E50K) mutation exhibit neurodegenerative phenotypes when derived from three-dimensional retinal organoids. Stem Cell Rep. *15*, 52–66.

VanderWall, K.B., Lu, B., Alfaro, J.S., Allsop, A.R., Carr, A.S., Wang, S., and Meyer, J.S. (2020b). Differential susceptibility of retinal ganglion cell subtypes in acute and chronic models of injury and disease. Sci. Rep. *10*, 17359.

VanderWall, K.B., Vij, R., Ohlemacher, S.K., Sridhar, A., Fligor, C.M., Feder, E.M., Edler, M.C., Baucum, A.J., 2nd, Cummins, T.R., and Meyer, J.S. (2019). Astrocytes regulate the development and maturation of retinal ganglion cells derived from human pluripotent stem cells. Stem Cell Rep. *12*, 201–212.

von Bartheld, C.S., Byers, M.R., Williams, R., and Bothwell, M. (1996). Anterograde transport of neurotrophins and axodendritic transfer in the developing visual system. Nature *379*, 830–833.

Wahlin, K.J., Maruotti, J.A., Sripathi, S.R., Ball, J., Angueyra, J.M., Kim, C., Grebe, R., Li, W., Jones, B.W., and Zack, D.J. (2017). Photoreceptor outer segment-like structures in long-term 3D retinas from human pluripotent stem cells. Sci. Rep. *7*, 766.

Whitmore, A.V., Libby, R.T., and John, S.W. (2005). Glaucoma: thinking in new ways-a rôle for autonomous axonal self-destruction and other compartmentalised processes? Prog. Retin. Eye Res. *24*, 639–662.

Xiang, M., Gan, L., Li, D., Chen, Z.Y., Zhou, L., O'Malley, B.W., Jr., Klein, W., and Nathans, J. (1997). Essential role of POU-domain factor Brn-3c in auditory and vestibular hair cell development. Proc. Natl. Acad. Sci. U S A *94*, 9445–9450.

Xiang, Y., Tanaka, Y., Cakir, B., Patterson, B., Kim, K.Y., Sun, P., Kang, Y.J., Zhong, M., Liu, X., Patra, P., et al. (2019). hESC-derived thalamic organoids form reciprocal projections when fused with cortical organoids. Cell Stem Cell *24*, 487–497.e487.

Yeh, M.L., Gonda, Y., Mommersteeg, M.T., Barber, M., Ypsilanti, A.R., Hanashima, C., Parnavelas, J.G., and Andrews, W.D. (2014). Robo1 modulates proliferation and neurogenesis in the developing neocortex. J. Neurosci. *34*, 5717–5731.

Zhong, X., Gutierrez, C., Xue, T., Hampton, C., Vergara, M.N., Cao, L.H., Peters, A., Park, T.S., Zambidis, E.T., Meyer, J.S., et al. (2014). Generation of three-dimensional retinal tissue with functional photoreceptors from human iPSCs. Nat. Commun. *5*, 4047.

Stem Cell Reports, Volume *16*

Supplemental Information

Extension of retinofugal projections in an assembled model of human pluripotent stem cell-derived organoids

Clarisse M. Fligor, Sailee S. Lavekar, Jade Harkin, Priya K. Shields, Kirstin B. VanderWall, Kang-Chieh Huang, Cátia Gomes, and Jason S. Meyer

Supplemental Table 1: Primary Antibodies Used in the Study

Antibody	Species	Company	Catalog Number	Dilution
Caspase-3	Rabbit	Promega	G7481	1:200
CHX10	Goat	Santa Cruz	SC-21690	1:200
CTIP2	Rat	Abcam	ab18465	1:500
Ki-67	Mouse	BD Biosciences	550609	1:500
OTX2	Goat	R&D Systems	AF1979	1:000
PAX6	Mouse	DSHB	PAX6	1:50
Recoverin	Rabbit	Millipore	AB5585	1:2000
S100β	Mouse	Abcam	ab11178	1:200
SATB2	Rabbit	Abcam	Ab34735	1:500
SOX2	Goat	R&D Systems	AF2018	1:1000
TCF7L2	Rabbit	Cell Signaling Technology	2569	1:200

Supplemental Figures

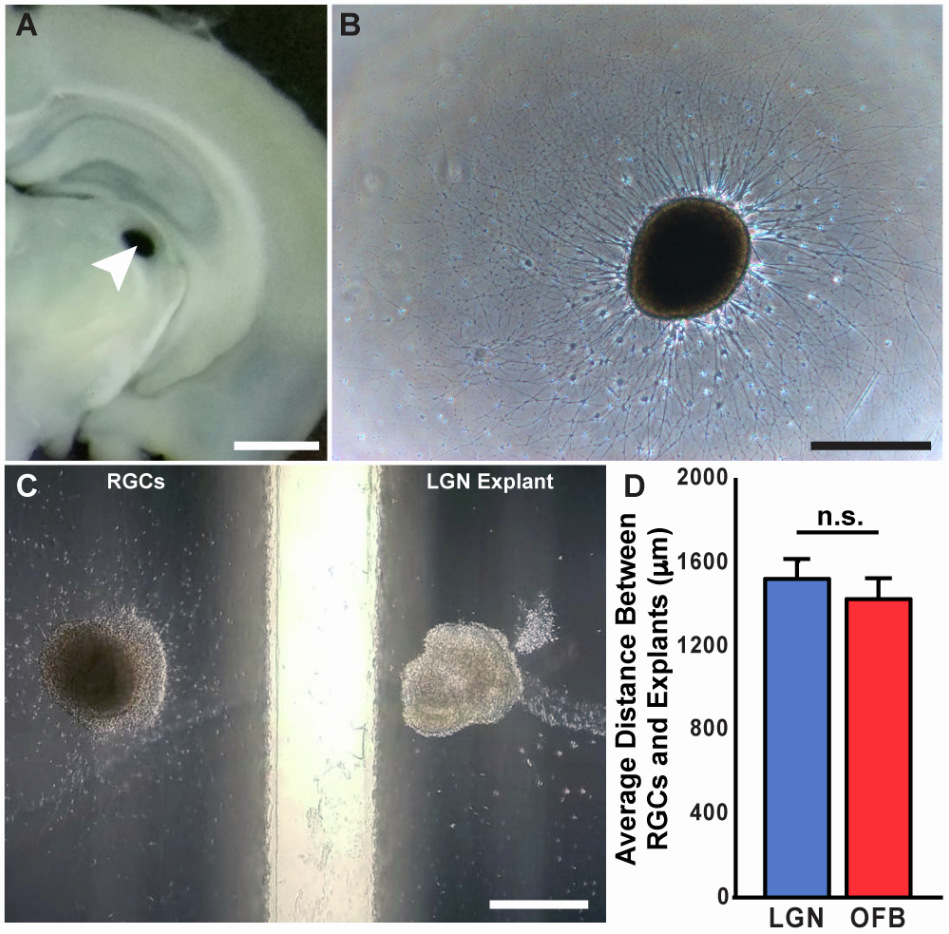

Supplemental Figure 1: **Establishment of co-cultures between retinal organoids and LGN or olfactory bulb explants.** (A) Explants were obtained from coronal sections of P1-P3 mouse brains, with explants from either LGN (pictured, arrowhead) or olfactory bulb extracted with a tissue punch. (B) Explant cultures of mouse LGN survived and extended lengthy neurites over the first week of growth. (C) Co-cultures were initially established between retinal organoids and explant cultures with a culture insert separating the two populations. (D) The distance between retinal organoids and either LGN or olfactory bulb explants was not significantly different across experiments. Scale bars equal 800 um in A, 200 um in B and C.

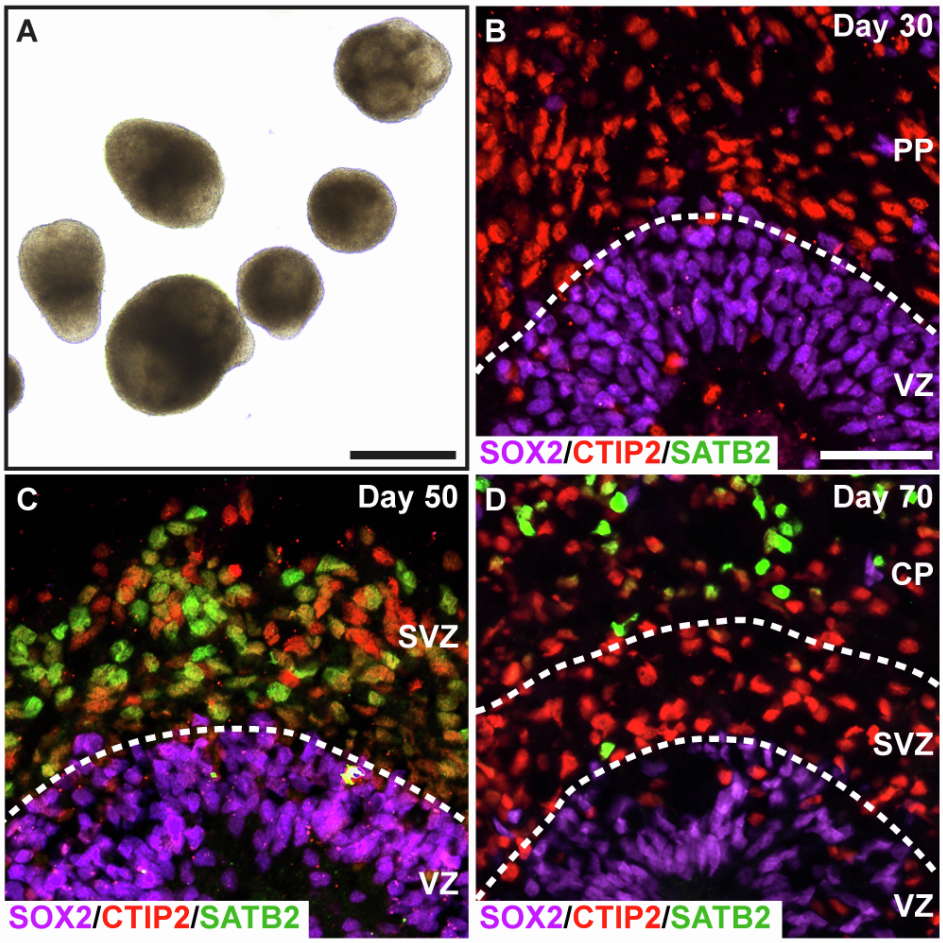

Supplemental Figure 2: **Differentiation of cortical organoids from hPSCs**. (A) Brightfield image of cortical organoids. (B-D) Sections through cortical organoids from 30-70 days of differentiation demonstrate primitive layering of cell types. PP = Preplate, VZ = Ventricular zone, SVZ = Subventricular zone, CP = Cortical plate. Scale bars = 1 mm in A, 25 um in B. Scale bar in B applies to C and D.

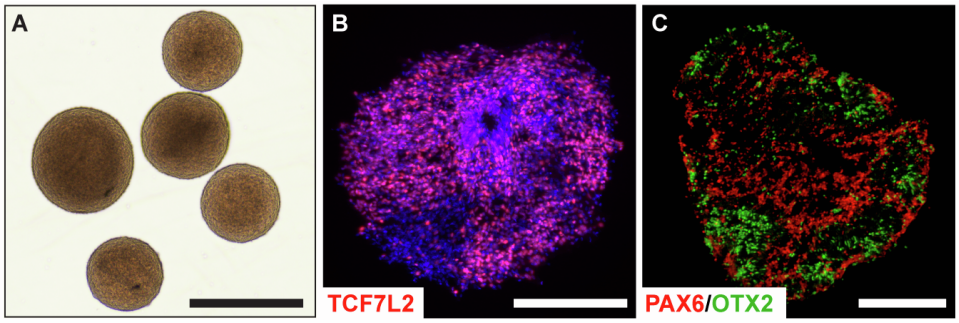

Supplemental Figure 3. Differentiation of thalamic organoids from hPSCs. (A) Brightfield image of thalamic organoids. (B-C) hPSC-derived thalamic organoids broadly express the thalamic-associated marker TCF7L2, as well as associated markers including PAX6 and OTX2.

Supplemental Experimental Procedures

Maintenance and Expansion of hPSCs

Undifferentiated cells were maintained and expanded as previously described (Fligor et al., 2020; Meyer et al., 2011), using Matrigel-coated 6-well plates and mTeSR1 medium (StemCell Technologies) until reaching approximately 70% confluency. Subsequently, cells were passaged using Dispase (2 mg/mL, Life Technologies) and split at a ratio of 1:6 every 4-5 days. Multiple lines of hPSCs were utilized in this study, including the H7, H9 and tiPS5 cell lines. Additionally, some of these lines were genetically modified to contain either a RGC-specific BRN3b:tdTomato reporter or a constitutive GFP reporter, as previously described (Sluch et al., 2017; VanderWall et al., 2020).

Differentiation of regional organoids

For retinal organoids, differentiation was initiated by lifting hPSCs from Matrigel-coated wells using Dispase (2 mg/mL). Cellular aggregates were maintained in suspension and gradually transitioned to a chemically defined neural induction medium (NIM), which consisted of DMEM/F12 (1:1), N2 supplement, MEM non-essential amino acids, heparin (2 ug/mL) and antibiotics. After 6 days, BMP4 (50 ng/ml) was added to induce retinal lineage differentiation. 2 days later, cellular aggregates were plated onto 6-well plates with 10% FBS to induce adhesion. Half media changes were performed on days 9 and 12 with a full media change occurring on day 15. After a total of 16 days of differentiation, cell aggregates were mechanically lifted and kept in suspension in Retinal Differentiation Medium (RDM), which consisted of DMEM/F12 (3:1), B27 supplement, MEM non-essential amino acids, and antibiotics. Retinal organoids were maintained in this medium until experimental time points indicated, and were screened for the expression of the BRN3:tdTomato reporter before use in subsequent analyses or to generate assembloids. Prosencephalic brain organoids were differentiated from hPSCs by excluding BMP4 from the medium at day 6 differentiation and EBs were plated on laminin-coated plates 2 days later, with all subsequent conditions maintained the same.

For differentiation of thalamic organoids, hPSCs were dissociated to a single cell suspension using Accutase for approximately 5 minutes. Single cells were resuspended in induction media (DMEM-F12, 15%

KSR, 1% MEM-NEAA, 1% Glutamax, 1% PSA and 100 μM β-Mercaptoethanol, 100 nM LDN-193189, 10 μM SB-431542, 4 μg/ml Insulin, 5% heat-inactivated FBS, and 50 μM Y27632) and aggregated in ultra-low-attachment 96-well plates (Nunc) at a density of 7,000 cells/well. Half media changes were performed every other day. After 8 days, aggregates were transferred to spinning culture (80 rpm/min) in 24-well low attachment plates (Corning) and maintained in patterning media (DMEM-F12, 0.15% Dextrose, 100 mM β-mercaptoethanol, 1% N2 supplement, 1% PSA, 2% B27 supplement minus vitamin A, 30 ng/ml BMP7 and 1 mM PD325901). Media was changed every other day until day 16, when differentiation media (1:1 mixture of DMEM-F12 and Neurobasal media, 0.5% N2 supplement, 1% B27 supplement, 0.5% MEM-NEAA, 1% Glutamax, 0.025% Insulin, 50 mM β-Mercaptoethanol, 1% PSA, 20 ng/ml BDNF and 200 mM ascorbic acid) with media changes every other day until day 25, and every four days thereafter.

Growth of hPSC-derived RGCs in microfluidic platforms

Retinal organoids were differentiated from hPSCs with an RGC-specific BRN3:tdTomato reporter, as previously described (Sluch et al., 2017; VanderWall et al., 2020). Within 45 days of differentiation, tdTomato-positive organoids were dissociated to single cells with Accutase and magnetically sorted with beads specific to the Thy1.2 cell surface antigen to yield a purified population of RGCs. These RGCs were then plated within microfluidic devices (Xona Microfluidics, XC450) at a density of 250,000 cells/device in BrainPhys medium (StemCell Technologies). To induce axonal recruitment into the contralateral chamber of each device, a volume differential between chambers was established, with the soma chamber containing 150 μl of BrainPhys medium, while the axonal compartment contained 100 μl, creating a net flow of medium toward the axonal chamber. Additionally, extra BDNF was added to the axonal chamber (total concentration 50 ng/ml) to recruit axons to cross over. Cultures were maintained in this state for up to 3 weeks, with media changes occurring every 2-3 days.

Animal Care and Brain Dissection

Pregnant female C57BL/6 mice were purchased from Jackson Laboratories (Bar Harbor, ME, http://www.jax.org) and housed within the animal care facility at the School of Science at Indiana University-Purdue University Indianapolis. Within the first 2 days after birth, mouse pups were anesthetized with

isofluourane and sacrificed by decapitation. Brains were then immediately dissected out and placed in a solution of artificial cerebrospinal fluid (aCSF). Coronal sections were then cut on a vibratome at a thickness of 300 μm and collected for analysis on a Leica A60 stereomicroscope to anatomically identify the lateral geniculate nuclei. Upon identification, the dorsal LGN was isolated with a 0.5 mm tissue punch (Electron Microscopy Sciences) and explant cultures were subsequently established. All experiments involving mice were approved by the Institutional Animal Care and Use Committee within the School of Science at Indiana University Purdue University Indianapolis and were conducted in accordance with the ARVO Statement for the Use of Animals in Ophthalmic and Vision Research.

Co-culture of RGCs and Mouse Brain Explants

To establish co-cultures between mouse LGN explants and hPSC-derived RGCs, a two-chambered silicone culture insert (Ibidi) allowed for the LGN and RGCs to be separated by at least 500 um. Any samples in which the LGN and RGC aggregates were more than 10 mm apart were excluded. Explants were plated into the left chamber of two-chamber culture inserts and allowed to adhere for 48 hours in RDM. hPSCs with a BRN3:tdTomato fluorescent reporter were differentiated as described above and after 40 days of differentiation, fluorescing organoids were chopped to a reproducible size of approximately 200 um with a tissue chopper (McIlwain) and plated in the adjacent chamber. Following adhesion of LGN and RGCs, culture inserts were manually removed to allow the growth of RGC neurites towards LGN explants. RGCs and LGN explants were co-cultured for one week before fixation in 4% paraformaldehyde, with tdTomato expression allowing for the identification of RGC neurites. As controls, some cultures consisted of only RGC-containing retinal organoid cultures, while other control experiments used RGCs in co-culture with mouse olfactory bulb explants, in which the olfactory bulb was dissected out of the brain and explants were cultures similarly to LGN explants.

Immunocytochemistry

For cryostat sectioning, organoids and assembloids were fixed with 4% paraformaldehyde, washed 3x in PBS, and then equilibrated in 20% and 30% sucrose solutions overnight at 4°C. After reaching equilibrium, organoids and/or assembloids were embedded in OCT and frozen on dry ice, and sections were then cut

at 90 um thickness on a cryostat. Similarly, co-cultures grown on coverslips were fixed in 4% paraformaldehyde and washed 3x in PBS before staining. Immunocytochemical staining of all samples was performed as previously described. Briefly, samples were permeabilized in 0.2% Triton X-100 for 10 minutes and subsequently blocked in 10% donkey serum for one hour at RT. Primary antibodies (Supplemental Table 1) were diluted in 0.1% Triton X-100 and 5% donkey serum. Following overnight incubation at 4°C, samples were washed in PBS and blocked with 10% donkey serum for 10 minutes. Secondary antibodies were diluted 1:1000 in 0.1% Triton X-100 and 5% donkey serum and incubated for 1 hour at RT. Finally, cells were washed with PBS and mounted onto slides for analysis.

Measurement of axonal outgrowth in assembloid cultures

Axonal outgrowth was examined in sections of assembloids cut at 90 um thickness at 3, 5, and 7 days post-assembly (dpa). RGC axons were identified by the expression of tdTomato within assembloids. The degree of axonal outgrowth was quantified following methods previously described for thalamic organoids (Xiang et al., 2019). Briefly, the ranges of axonal outgrowth were classified into 3 categories: not approaching the midline of targeted organoid (r1), already crossing the midline of targeted organoid (r2), and already approaching the opposite tip of the targeted organoid (r3). 30 assembloids were generated and examined for each experiment, with 10 assembloids analyzed per timepoint. The percentage of axons extending to various ranges at specified timepoints were quantified for each experiment.

Growth Factor Array

Growth Factor Array analysis was performed using the C-Series Human Cytokine Antibody Array C1000 (RayBiotech #AAh-CYT-1000-2) following manufacturer's instructions. Briefly, brain organoids were lysed in the provided lysis buffer and diluted to a concentration of 500 ug/mL using the provided blocking buffer. Antibody membranes were subsequently blocked for 30 minutes at RT. After removal of blocking buffer, 1 mL of diluted sample was added to antibody membranes and incubated overnight at 4°C. The following day, membranes were washed with provided buffers and incubated with appropriate biotinylated antibody cocktails overnight at 4°C. The following day, membranes were once again washed and incubated in 1X HRP-Streptavidin for 2 hours at RT. Following a final wash, membranes were transferred onto blotting

paper and incubated in the provided detection buffer for 2 minutes at RT. Finally, dot blots were imaged using a chemiluminescence imaging system (Odyssey CLX, LiCor) and analyzed using the gel analysis function in Image J.

Statistical Analyses

For measurements of axonal outgrowth within microfluidic platforms, the number of axons entering the axonal compartment was quantified at 3, 5 and 7 days post plating. Multiple replicates (n=5) were obtained at each time point. A student's two-tailed t-test using the Holm-Sidak method determined significance between + and – BDNF, with *p* values less than 0.05 considered significant.

In order to analyze and quantify the effects of co-culturing RGCs with or without explant targets, RGC neurites were identified by tdTomato expression and neurites were traced using a semi-automatic ImageJ plug-in, NeuronJ. The mean length of neurites in each condition were calculated along with the standard error of the mean. One-way ANOVA statistical analyses at 95% confidence (post-hoc Tukey) was performed to determine significance compared to controls. Statistical significance was determined based on a *p* value less than 0.05. Sholl analysis was performed to determine complexity of neurite outgrowth. The number of neurites crossing each ring was quantified for each condition indicated (n=9). Grubb's test was used to remove outliers with an alpha of 0.05. One-way ANOVA followed by Tukey's post hoc or student's two-tailed t-test using the Holm-Sidak method determined significance between samples, with *p* values less than 0.05 considered significant. To determine specificity of outgrowth, the longest neurite in 10 degree sections was measured and compared to average neurite lengths of controls. One-way ANOVA statistical analyses at 95% confidence (post hoc Tukey) was performed, excluding outliers, to determine significance compared to the control. Statistical significance was determined based on a *p* value less than 0.05.

Within assembloid cultures, range index examination was calculated and significance was determined with a one-way ANOVA to compare each range at the time points indicated. Statistical significance was determined based on a *p* value less than 0.05.To determine the long-term effects of assembloids upon organoid growth, the retinal area and TdTomato intensity of retinal organoids was measure using FIJI ImageJ. Grubb's test was used to remove outliers with an alpha of 0.05. One-way

ANOVA followed by Tukey's post hoc determined significance compared to control. For proliferation and apoptosis studies, the overall area of Ki67 or Caspase-3 was measured and compared to controls using a student's two-tailed t-test using the Holm-Sidak method. A one-way ANOVA was once again used to determine the effectiveness of BDNF treatment on retinal organoids. For all tests, a p value of 0.05 was used was used to determine statistical significance. In order to analyze outgrowth within thalamic organoids, the number of axons crossing after just 3 days of fusion was quantified. A student's two-tailed t-test using the Holm-Sidak method determined significance between samples, with p values less than 0.05 considered significant. All statistical analyses were performed using Graphpad Prism software.

Supplemental References:

Fligor, C.M., Huang, K.C., Lavekar, S.S., VanderWall, K.B., and Meyer, J.S. (2020). Differentiation of retinal organoids from human pluripotent stem cells. Methods Cell Biol *159*, 279-302.

Meyer, J.S., Howden, S.E., Wallace, K.A., Verhoeven, A.D., Wright, L.S., Capowski, E.E., Pinilla, I., Martin, J.M., Tian, S., Stewart, R.*, et al.* (2011). Optic vesicle-like structures derived from human pluripotent stem cells facilitate a customized approach to retinal disease treatment. Stem Cells *29*, 1206-1218.

Sluch, V.M., Chamling, X., Liu, M.M., Berlinicke, C.A., Cheng, J., Mitchell, K.L., Welsbie, D.S., and Zack, D.J. (2017). Enhanced Stem Cell Differentiation and Immunopurification of Genome Engineered Human Retinal Ganglion Cells. Stem Cells Transl Med *6*, 1972-1986.

VanderWall, K.B., Huang, K.C., Pan, Y., Lavekar, S.S., Fligor, C.M., Allsop, A.R., Lentsch, K.A., Dang, P., Zhang, C., Tseng, H.C.*, et al.* (2020). Retinal Ganglion Cells With a Glaucoma OPTN(E50K) Mutation Exhibit Neurodegenerative Phenotypes when Derived from Three-Dimensional Retinal Organoids. Stem Cell Reports *15*, 52-66.

Xiang, Y., Tanaka, Y., Cakir, B., Patterson, B., Kim, K.Y., Sun, P., Kang, Y.J., Zhong, M., Liu, X., Patra, P.*, et al.* (2019). hESC-Derived Thalamic Organoids Form Reciprocal Projections When Fused with Cortical Organoids. Cell Stem Cell *24*, 487-497.e487.